## Title

# Higgsino Dark Matter Confronts 14 Years of Fermi γ-Ray Data



## Journal

Physical Review Letters, 130(20)

## ISSN

0031-9007

## Authors

Dessert, Christopher
Foster, Joshua W
Park, Yujin
et al.

## Publication Date

2023-05-19

## DOI

10.1103/physrevlett.130.201001

# Higgsino Dark Matter Confronts 14 Years of Fermi $\gamma$-Ray Data

Christopher Dessert,[1,2,3] Joshua W. Foster,[4] Yujin Park,[1,2] Benjamin R. Safdi,[1,2] and Weishuang Linda Xu[1,2]
[1]*Berkeley Center for Theoretical Physics, University of California, Berkeley, California 94720, USA*
[2]*Theoretical Physics Group, Lawrence Berkeley National Laboratory, Berkeley, California 94720, USA*
[3]*Leinweber Center for Theoretical Physics, Department of Physics, University of Michigan, Ann Arbor, Michigan 48109 USA*
[4]*Center for Theoretical Physics, Massachusetts Institute of Technology, Cambridge, Massachusetts 02139, USA*

(Received 30 July 2022; revised 13 October 2022; accepted 25 April 2023; published 16 May 2023)

Thermal Higgsino dark matter (DM), with mass around 1 TeV, is a well-motivated, minimal DM scenario that arises in supersymmetric extensions of the standard model. Higgsinos may naturally be the lightest superpartners in split-supersymmetry models that decouple the scalar superpartners while keeping Higgsinos and gauginos close to the TeV scale. Higgsino DM may annihilate today to give continuum $\gamma$-ray emission at energies less than a TeV in addition to a linelike signature at energies equal to the mass. Previous searches for Higgsino DM, for example with the H.E.S.S. $\gamma$-ray telescope, have not reached the necessary sensitivity to probe the Higgsino annihilation cross section. In this work we make use of 14 years of data from the *Fermi* Large Area Telescope at energies above $\sim$10 GeV to search for the continuum emission near the Galactic Center from Higgsino annihilation. We interpret our results using DM profiles from Milky Way analog galaxies in the FIRE-2 hydrodynamic cosmological simulations. We set the strongest constraints to date on Higgsino-like DM. Our results show a mild, $\sim 2\sigma$ preference for Higgsino DM with a mass near the thermal Higgsino mass and, depending on the DM density profile, the expected cross section.

DOI: 10.1103/PhysRevLett.130.201001

Dark matter (DM) makes up $\sim$27% of the energy in our Universe today [1], with only $\sim$5% of the energy density in ordinary matter, yet its microscopic nature remains unknown. One tantalizing possibility, which has driven decades of experimental and theoretical effort, is that DM arises as the lightest superpartner (LSP) in supersymmetric (SUSY) extensions of the standard model that address the hierarchy problem related to the unnaturally low Higgs mass parameter (see Ref. [2] for a review). LSP DM at the $\sim$TeV scale may naturally acquire the correct DM abundance through thermal freeze-out. On the other hand, electroweak scale SUSY and LSP DM have come under increasing tension in recent years from null searches for new physics at the Large Hadron Collider (LHC) [3,4], direct detection experiments [5], and indirect searches [6,7].

Natural LSP candidates are the neutral gauginos—namely, bino and wino LSPs—and the Higgsino. Pure bino DM is excluded by direct searches at the LHC [8,9]. Wino DM is in strong tension with null results from DM annihilation searches with the H.E.S.S. $\gamma$-ray telescope [6,10]. Nearly pure Higgsino LSPs, on the other hand, remain one of the better motivated and sought after, yet unprobed, DM scenarios (see, e.g., Ref. [11] for a recent summary). Higgsinos, which are the superpartners of the two Higgs doublets in the minimal supersymmetric standard model (MSSM), are especially motivated in light of (i) null results for wino DM and (ii) the fact that null searches for superpartners at, e.g., the LHC suggest that nature may implement a split-spectrum version of SUSY such as split-SUSY [12–16], which naturally leads to Higgsino or wino LSP DM. Split-SUSY, mini-split, and similar constructions [17] aim to preserve LSP DM and high-scale gauge unification but give up on trying to fully solve the hierarchy problem (see Ref. [18] for a review of the hierarchy problem); in such models the scalar superpartners are taken to have large masses, with the gauginos and Higgsinos remaining near the TeV scale. Such split-spectrum models may accommodate the observed Higgs mass and solve a number of troublesome problems with the MSSM, such as the lack of flavor changing neutral currents [19] and the nonobservation of new *CP* violation in electric dipole moment searches [20,21].

In this work we search for annihilation signatures of Higgsino DM with *Fermi* Large Area Telescope (LAT) $\gamma$-ray data. The Higgsino interacts with ordinary matter through the electroweak force. In this model the Higgsino was thermally coupled with the standard model plasma at early times. As the Universe expands and cools down, the Higgsinos freeze out of thermal equilibrium and behave like cold DM thereafter. The requirement that freeze-out produces the correct DM abundance fully determines the Higgsino mass. Moreover, the Higgsino is invisible to present-day direct detection experiments for the reasons given below. The Higgsino mass arises from the Lagrangian term $\mathcal{L} \supset -\mu \tilde{H}_u \cdot \epsilon \cdot \tilde{H}_d + \mathrm{H.c.}$, where $\mu$ is the MSSM $\mu$ parameter, $\tilde{H}_u$ ($\tilde{H}_d$) is the up-type (down-type) Higgsino electroweak doublet, and $\epsilon$ is the totally antisymmetric symbol in $\mathrm{SU}(2)_L$ space. There are two neutral Higgsino fermions, which are generically split into two nondegenerate Majorana mass eigenstates by dimension-five operators that have the effect of inducing a slight mixing between the neutral gauginos and Higgsinos (see, e.g., Ref. [22]). The charged Higgsino states are heavier than the neutral states by at least ~350 MeV because of radiative contributions to the charged Higgsino masses below electroweak symmetry breaking [23]. The mass splitting between the two neutral Majorana states, which we call $\Delta m$, must be greater than around 200 keV to avoid direct detection constraints from inelastic scattering through the exchange of a Z boson, where the lower Majorana state scatters into the heavier mass eigenstate (see, e.g., Ref. [22]). When $\Delta m \gtrsim 200$ keV, direct detection of Higgsino DM proceeds through elastic scattering with higher-dimensional operators and is thought to be below the neutrino floor, which is the direct detection cross section below which neutrinos become a virtually irreducible source of background [24–27].

The relic abundance of Higgsinos from thermal freeze-out matches the observed DM abundance [1] for mass $m_\chi = 1.08 \pm 0.02$ TeV, accounting for uncertainties on the DM abundance [28]. We refer to the Higgsino with such a mass as the thermal Higgsino. Apart from the SUSY motivations, Higgsino DM may be viewed through the lens of minimal DM [29]. The strongest existing indirect detection constraints on the thermal Higgsino arise from Galactic Center (GC) searches for the line emission expected due to the $\gamma\gamma$ and $\gamma Z$ final states with H.E.S.S. [30], which constrain $\langle \sigma v \rangle_{\gamma\gamma} \lesssim 4 \times 10^{-28}$ cm$^{-3}$/s assuming an Einasto DM profile, whereas the thermal cross section is a factor of 4 smaller, and for H.E.S.S. searches for continuum emission from annihilation to $W^+W^-$ [31]. The forthcoming Cherenkov Telescope Array (CTA), on the other hand, with 500 hours of exposure, is expected to have sensitivity to Higgsino DM at the thermal mass [32]. Future lepton or hadron colliders may also be able to discover thermal Higgsinos [33–35]. Potential discovery via next-generation direct detection experiments on the other hand is comparatively difficult, due to the fact that elastic scattering for all presently viable Higgsino models is expected to be suppressed below the neutrino floor [28].

In this Letter we use the existing 14 years of data from the *Fermi* LAT to achieve world-leading sensitivity to Higgsino DM by searching for annihilation to continuum gamma rays through the $W^+W^-$ and $ZZ$ final states. Our upper limits on the annihilation cross section surpass those from H.E.S.S. for Higgsino-like DM with mass $m_\chi \sim$ TeV, though our upper limits are weaker than expected due to the presence of a modest (~$2\sigma$) preference for the signal model over the null hypothesis. We interpret our results in the context of DM profiles from the FIRE-2 hydrodynamic cosmological simulations [36,37] to show that the best-fit annihilation cross section we recover may be consistent with the expected Higgsino cross section, potentially providing the first hint of thermal Higgsino DM.

*Data reduction and analysis.*—We reduce 722 weeks of Pass 8 *Fermi* $\gamma$-ray data with SOURCE selection criterion taken between August 4, 2008, and June 10, 2022, with the recommended quality cuts DATAQUAL $> 0$ and LATCONFIG $== 1$ along with zenithangle less than 90°. We include the top three of four quartiles of the data as ranked by the point spread function. As in Ref. [38], we initially bin the data into 40 logarithmically spaced energy bins between 200 MeV and 2 TeV, and we bin spatially using HEALPIX [39] with nside $= 512$. However, in our analysis we only analyze data starting in the 18th energy bin, with minimum energy ~10.02 GeV, since our signal peaks at higher energies and since the lower energies are more contaminated by Galactic diffuse emission. Starting at 10 GeV we also mostly avoid the *Fermi* Galactic Center excess, which is an excess of ~GeV gamma rays observed near the GC [40–45]; the excess has not been found to extend above 10 GeV with our Galactic emission model [46]. We include energies up to the DM mass $m_\chi$, as the signal spectrum has no support beyond that.

Our region of interest (ROI) for the analysis is that within 10° of the GC, with the Galactic plane masked ($|b| \geq 1°$) in addition to a 4FGL-DR3 point source (PS) mask [47,48], which is described in the Supplemental Material [49]. We then further divide our ROI into nine concentric annuli, going out to 10° from the GC starting at 1°, with angular spacings of 1°. We stack and analyze the spectral data in each of these annuli independently. The photon counts in our analysis ROI above 10 GeV are illustrated in the top panel of Fig. 1.

We model the spectral data in each annulus under the null hypothesis using a linear combination of (i) the spectral template derived from the *Fermi* Galactic emission model gll_iem_v07 (p8r3), which also accounts for emission from the *Fermi* bubbles, reprocessed for our dataset and selection criterion; (ii) the 4FGL-DR3 PS spectral template appropriate for our ROI; and (iii) the isotropic diffuse emission appropriate for our Galactic emission model and dataset. PS and isotropic emission, however, are subdominant compared with Galactic diffuse emission, as illustrated in the Supplemental Material [49], Fig. S1. Spatial-spectral models for each component are generated accounting for the instrumental response using the

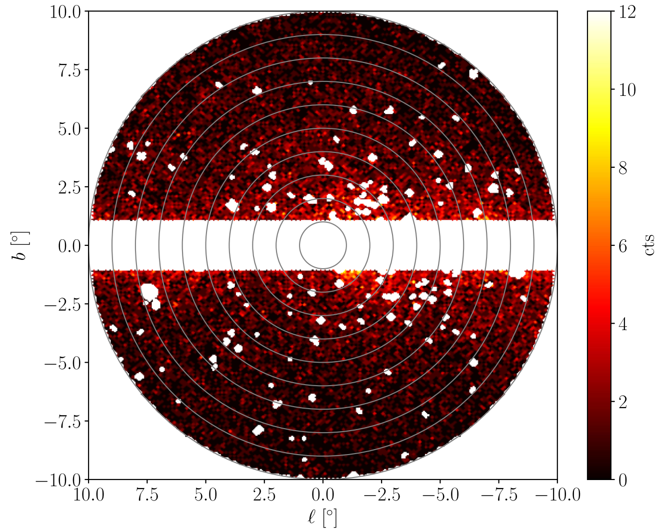


FIG. 1. The photon count data used in this work in our ROI, which has the Galactic plane masked at $|b| \geq 1°$ along with 4FGL-DR3 PSs and pixels more than 10° from the GC. For illustration the data are summed above 10 GeV. We analyze the data in nine concentric annuli, as indicated.

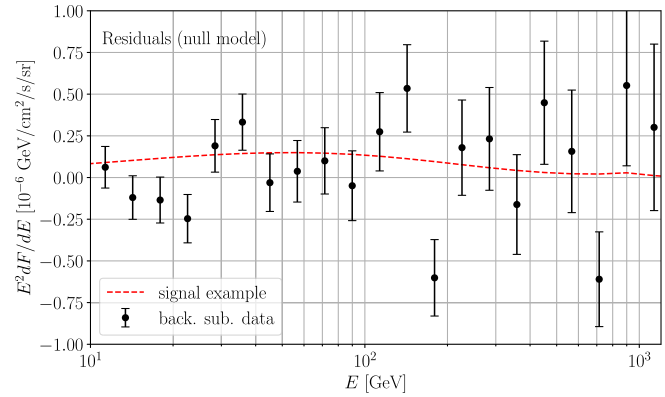


FIG. 2. The data with the best-fit null hypothesis model subtracted and then summed over all annuli. For reference we illustrate a Higgsino-like signal with $m_\chi = 1.1$ TeV, $\langle \sigma v \rangle = 5 \times 10^{-26}$ cm$^3$/s, and a NFW DM profile.

gtsrcmaps and gtmodel functions in Fermitools. We define the ensemble of null-hypothesis spectral models (Galactic emission, PS, and isotropic) as the background templates. In each radial bin we construct a likelihood to constrain the spectral model, which consists of the background templates along with the signal template that is discussed shortly, by taking the product of the Poisson probabilities to observe the data counts in each energy bin given the model prediction. The background templates are given individual nuisance parameters that rescale the overall normalization of that template; we require the nuisance parameters to be positive. At a given DM mass $m_\chi$ and in a given radial annulus, we construct the profile likelihood for the annihilation cross section $\langle \sigma v \rangle$ profiling over the background nuisance parameters. We then construct the joint profile likelihood for $\langle \sigma v \rangle$, at fixed $m_\chi$, by taking the product of the profile likelihoods over all radial bins. (See the Supplemental Material [49] for details, along with an alternative analysis that incorporates spatial information into the likelihood.)

In Fig. 2 we show the background-subtracted counts data, with the best-fit null hypothesis model, summed over all annuli up through 1.1 TeV for an analysis looking for a Higgsino with $m_\chi = 1.1$ TeV. The data are largely consistent with the null hypothesis. Note that this figure is for illustrative purposes only and is not used in the analysis, which treats the radial bins separately. Our sensitivity is dominated by the energy bins less than around 100 GeV; this should be contrasted with the sensitivity of upcoming experiments like CTA that will probe thermal Higgsino DM at energies near a TeV but lose sensitivity below ~100 GeV. Our inclusion of photons with energies between ~10 and 100 GeV is what makes us competitive with CTA, even though CTA will have a much larger effective area than *Fermi*.

*Results.*—To interpret the data in the context of the Higgsino model we need to compute the $\gamma$-ray spectrum $dN/dE$ per annihilation from the decays of the unstable particles produced during Higgsino annihilation. The dominant annihilation channels are $\chi\chi \to W^+W^-$ and $\chi\chi \to ZZ$. At $m_\chi = 1.1$ TeV the branching ratio to $W$ (Z) pairs is ~60% (~40%). Since the Higgsino annihilates through its electroweak interactions, for a given $m_\chi$ there is a fixed and calculable $\langle \sigma v \rangle$. This annihilation cross section is illustrated in Fig. 3 as a function of $m_\chi$. The $dN/dE$ for annihilations to $W$ and Z pairs are calculated using PPPC 4 DM ID [58]. When constraining the Higgsino model we treat the overall cross section $\langle \sigma v \rangle$ as a free parameter, which could be negative, but with the branching ratio to $W$ and Z pairs fixed.

In addition to the spectrum per annihilation we also need to know the astrophysical $J$ factor, $J \equiv \int ds \rho_{\rm DM}^2(s)$, in our ROI in order to compute the expected signal in our radial annuli. Here, $\rho_{\rm DM}(s)$ is the DM density along the line of sight, parametrized by the distance $s$ from Earth. Our benchmark DM profile is the spherically symmetric Navarro–Frenk–White (NFW) [59,60] profile, normalized to produce a local DM density $\rho_{\rm DM}(s=0) = 0.4$ GeV/cm$^3$, with a scale radius $r_s = 20$ kpc, and with the distance from the GC to the Sun of $r_\odot = 8.23$ kpc [61]. Our local DM density choice is motivated by the recent review [62], which concludes that local DM density measurements, from analyses of stellar motions perpendicular to the disk within a few kpc, tend to favor the range 0.4–0.6 GeV/cm$^3$, broadly consistent with rotation curve data, though one should keep in mind that the true local DM density may be slightly larger or smaller than our choice. Furthermore, the scale radius is currently poorly

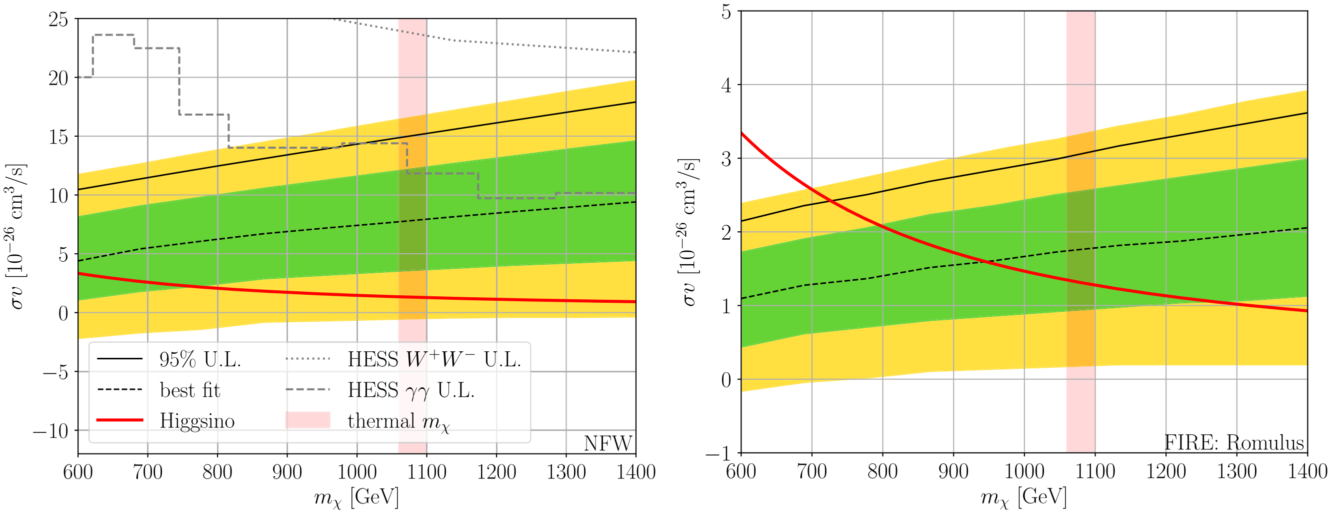


FIG. 3. The best-fit annihilation cross section for Higgsino-like DM as a function of the DM mass for our fiducial analysis assuming a NFW DM profile (left) and the FIRE-2 Romulus profile (right), which gives the best fit to the data of all profiles considered. We illustrate the best fit, $1\sigma$ (green) and $2\sigma$ (gold) confidence intervals for the recovered cross section, in addition to the 95% one-sided upper limit. We compare our results to the expected Higgsino annihilation cross section (red) and to the 95% upper limits from the H.E.S.S. searches for annihilation to $W^+W^-$ and $\gamma$-ray lines. The $m_\chi$ range, accounting for uncertainties, where Higgsinos make up the correct DM abundance in the standard thermal cosmology is shaded (thermal $m_\chi$). For the Romulus profile the recovered cross section is consistent with the expected cross section for the thermal Higgsino within $1\sigma$ (green band) and inconsistent with the null hypothesis of no Higgsino at $\sim 2\sigma$, as illustrated by the gold band. Note that $\langle\sigma v\rangle$ is allowed to be both positive and negative in the analysis, even though negative cross sections are unphysical. For all $m_\chi$ we assume that Higgsinos make up all of the observed DM.

constrained, such that $r_s = 20$ kpc represents a reasonable choice as opposed to a value strongly preferred by data.

Given the *ad hoc* nature of the NFW profile, and that it is motivated by DM-only $N$-body simulations, a potentially more promising approach to computing the $J$-factor profiles is to use the results for Milky Way analog galaxies in hydrodynamic cosmological simulations that include baryonic effects. Toward that end, we also compute the $J$-factor profiles in 12 FIRE-2 enlarged Milky Way analog galaxies [36], using simulation outputs provided in Ref. [37]. The FIRE-2 simulations are state-of-the-art hydrodynamic simulations, which provide the highest angular resolution to date for $J$-factor profiles, that incorporate, e.g., stellar feedback and radiative transfer amongst baryons, which dominate the inner potential wells of Milky Way sized galaxies, in addition to gravitational dynamics. Six of these twelve galaxies, including Romulus and Romeo which we discuss more below, were evolved in pair configurations to mimic the interactions between the Milky Way and Andromeda. The Milky Way analogs are chosen to have stellar masses in the range $(3, 11) \times 10^{10} M_\odot$ with virial masses in $(0.9, 1.8) \times 10^{12} M_\odot$ [37]. The particle masses and positions were then adjusted in Ref. [37] such that the local DM density is $0.38\ \mathrm{GeV/cm^3}$ at the distance to the Sun $r_\odot = 8.3$ kpc, which are similar to our fiducial values for the NFW profile. We then compute the azimuthally averaged $J$ factors in our ROI annuli; these $J$ factors are compared to those from the NFW profile in the Supplemental Material [49], Fig. S5.

In the left panel of Fig. 3 we show the results of our analysis of the *Fermi* data interpreted for Higgsino DM using the NFW DM profile. We illustrate the best-fit cross section, along with 1 and $2\sigma$ significance containment intervals, as functions of the Higgsino mass, assuming that at each mass the Higgsino makes up all of the DM (see the Supplemental Material [49], Fig. S10, for our results assuming a subfraction of the DM). Our one-sided 95% upper limit is also illustrated. For the fiducial NFW profile we are unable to exclude the Higgsino cross sections over the mass range shown. At the thermal mass the local significance in favor of the signal model is $\sim 2\sigma$ (see the Supplemental Material [49], Fig. S8). Since the spectral shape of the signal is not strongly dependent on the Higgsino mass, we are not able to further constrain $m_\chi$. Note that in Fig. 2 we illustrate the Higgsino model prediction relative to the background-subtracted and fully stacked data for a reference cross section. We find no evidence for mismodeling, as is quantified in Table S1, which provides a list of $p$ values associated with the signal and null hypothesis fits in each annuli.

The FIRE-2$J$-factor profiles are typically enhanced relative to that of the NFW model due to adiabatic contraction, as illustrated in the Supplemental Material [49], Fig. S5, though there is significant spread over the 12 realizations. In the right panel of Fig. 3 we show our results interpreted in the context of the FIRE-2 halo, Romulus, with the largest $J$ factor (the other halos are illustrated in the Supplemental Material [49]). Note that we use the FIRE-2 naming conventions for the Milky Way analog galaxies [36]. The FIRE-2 halo profiles lead to comparable discovery significances compared with the NFW analysis, as illustrated in the Supplemental Material [49], Fig. S8, with Romulus providing the best fit. Intriguingly, with the Romulus profile and multiple other FIRE-2 profiles the excess in favor of the signal model has a best-fit cross section consistent with the Higgsino model at the thermal mass. (As seen in Fig. 3, the best-fit cross section is slightly higher than the predicted Higgsino cross section for the Romulus profile, implying that the expected significance in favor of the signal model, $\sim 1.6\sigma$, is slightly lower than the observed value $\sim 2.2\sigma$.) Over the ensemble of 12 FIRE-2$J$-factor profiles that we consider, the best-fit $\langle \sigma v \rangle$ for $m_\chi \approx 1.08$ TeV ranges from $1.7 \times 10^{-26}$ cm$^3$/s to $7.3 \times 10^{-26}$ cm$^3$/s, with the median value of $3.4 \times 10^{-26}$ cm$^3$/s; the Higgsino cross section at this mass is $\langle \sigma v \rangle \approx 1.3 \times 10^{-26}$ cm$^3$/s. The Romulus profile leads to the best-fit cross section at $m_\chi \approx 1.08$ TeV of $\langle \sigma v \rangle = 1.7 \pm 0.8 \times 10^{-26}$ cm$^3$/s. The Romeo halo may be the most Milky Way-like, due to the similarities of its thick disk, circular velocity, and stellar mass to the Milky Way; using this halo we recover a cross section $\langle \sigma v \rangle = 1.9 \pm 1.0 \times 10^{-26}$ cm$^3$/s at the thermal Higgsino mass. We caution that the FIRE-2 profiles are expected to have resolution down to $\sim 2.75°$, and thus our results in the inner two annuli could be subject to simulation error, in particular, underestimates of the $J$ factors [37]. In the Supplemental Material [49], however, we show that we find comparable results when excluding the inner rings.

In Fig. 3 (left) we show the 95% upper limit from an analysis of H.E.S.S. data looking for continuum emission above $\sim 200$ GeV associated with $\chi\chi \to W^+W^-$ [31]. H.E.S.S. is less sensitive to $\chi\chi \to ZZ$, since annihilation to Z pairs produces significantly fewer photons above $\sim 200$ GeV than annihilation to $W$ pairs, so to convert the results presented in Ref. [31] to Higgsino-like DM limits we use only the $W^+W^-$ result (additionally, H.E.S.S. does not present results for annihilation to Z pairs). Furthermore, Ref. [31] uses a ROI ranging from 0.5° to 2.9° from the GC and assumes an Einasto profile; we rescale their results to those appropriate for a NFW profile in the left panel of Fig. 3. The H.E.S.S. upper limits are less constraining than our upper limits across the mass range shown. (The FIRE-2 simulations do not have resolution down to $\sim 0.5°$, so we do not show the results from Ref. [31] in the right panel of Fig. 3).

Constraints on Higgsino DM using H.E.S.S. searches for $\gamma$-ray lines, which are from the loop-suppressed processes $\chi\chi \to \gamma\gamma$ and $\chi\chi \to Z\gamma$, are also relevant, though the hard-photon spectrum is affected by electroweak radiative effects [63]. We translate the H.E.S.S. $\gamma$-ray line limits in Ref. [30], which were computed using the same ROI as in their continuum $W^+W^-$ search described above, to limits on the total annihilation cross section using the next-to-leading logarithmic prime calculation for the energy spectrum near the $\gamma$-ray endpoint in Ref. [63] (see also Ref. [64]); the recasted limit is illustrated in the left panel of Fig. 3. The H.E.S.S. upper limit surpasses our upper limit at large masses, though it should be kept in mind that the H.E.S.S. analysis is significantly closer to the GC than ours, and thus the comparison relies on the possibly incorrect shape of the NFW profile.

*Discussion.*—In this work we set the strongest constraints to date on Higgsino-like DM that annihilates to $W^+W^-$ and $ZZ$ using nearly the entire *Fermi* dataset collected since the mission's launch in 2008. We search for the continuum $\gamma$-ray emission above 10 GeV associated with the decays of these massive vector bosons. We find a modest ($\sim 2\sigma$) preference for the Higgsino model over the null hypothesis of background-only emission. The best-fit cross section is consistent with the expected Higgsino cross section for a thermal ($m_\chi \approx 1.1$ TeV) Higgsino making up all of the DM for multiple FIRE-2 DM density profiles. Given that Higgsino DM is well motivated from supersymmetry, the possibility that the data present the first hint for Higgsino DM is promising. This possibility will be tested with the upcoming CTA [32], which should be sensitive to Higgsino DM annihilation.

The supporting data for this Letter, including a data cube containing the log-likelihood values that go into our results, are openly available from [65].

We thank Dan Hooper, Simon Knapen, Matthew McCullough, Lina Necib, Nick Rodd, Tracy Slatyer, and Tim Cohen for useful discussions, and we thank Daniel McKeown and the FIRE-2 project for providing us with the simulated halo profiles used in our analysis. J. W. F was supported by a Pappalardo Fellowship. C. D., Y. P., and B. R. S. were supported in part by the DOE Early Career Grant No. DESC0019225. W. L. X. thanks the Mainz Institute of Theoretical Physics of the Cluster of Excellence PRISMA+ (Project ID No. 39083149) for its hospitality during completion of part of this work, and is supported by the U.S. Department of Energy under Contract No. DE-AC02-05CH11231. This research used resources from the Lawrencium computational cluster provided by the IT Division at the Lawrence Berkeley National Laboratory, supported by the Director, Office of Science, and Office of Basic Energy Sciences, of the U.S. Department of Energy under Contract No. DE-AC02-05CH11231.

[1] N. Aghanim *et al.* (Planck Collaboration), Planck 2018 results. VI. Cosmological parameters, Astron. Astrophys. **641**, A6 (2020); Astron. Astrophys. **652**, C4(E) (2021).

[2] Gerard Jungman, Marc Kamionkowski, and Kim Griest, Supersymmetric dark matter, Phys. Rep. **267**, 195 (1996).

[3] Serguei Chatrchyan *et al.* (CMS Collaboration), Interpretation of searches for supersymmetry with simplified models, Phys. Rev. D **88**, 052017 (2013).

[4] Georges Aad *et al.* (ATLAS Collaboration), Summary of the ATLAS experiment's sensitivity to supersymmetry after LHC Run 1—interpreted in the phenomenological MSSM, J. High Energy Phys. 10 (2015) 134.

[5] E. Aprile *et al.* (XENON Collaboration), Dark Matter Search Results from a One Ton-Year Exposure of XENON1T, Phys. Rev. Lett. **121**, 111302 (2018).

[6] Timothy Cohen, Mariangela Lisanti, Aaron Pierce, and Tracy R. Slatyer, Wino dark matter under siege, J. Cosmol. Astropart. Phys. 10 (2013) 061.

[7] A. Albert *et al.* (Fermi-LAT and DES Collaborations), Searching for dark matter annihilation in recently discovered Milky Way satellites with Fermi-LAT, Astrophys. J. **834**, 110 (2017).

[8] Georges Aad *et al.* (ATLAS Collaboration), Search for squarks and gluinos with the ATLAS detector in final states with jets and missing transverse momentum using $\sqrt{s} = 8$ TeV proton–proton collision data, J. High Energy Phys. 09 (2014) 176.

[9] Vardan Khachatryan *et al.* (CMS Collaboration), Searches for supersymmetry using the $M_{T2}$ variable in hadronic events produced in pp collisions at 8 TeV, J. High Energy Phys. 05 (2015) 078.

[10] JiJi Fan and Matthew Reece, In wino veritas? Indirect searches shed light on neutralino dark matter, J. High Energy Phys. 10 (2013) 124.

[11] Raymond T. Co, Benjamin Sheff, and James D. Wells, Race to find split Higgsino dark matter, Phys. Rev. D **105**, 035012 (2022).

[12] James D. Wells, Implications of supersymmetry breaking with a little hierarchy between gauginos and scalars, in *11th International Conference on Supersymmetry and the Unification of Fundamental Interactions* (2003), arXiv:hep-ph/0306127.

[13] G. F. Giudice and A. Romanino, Split supersymmetry, Nucl. Phys. **B699**, 65 (2004); Nucl. Phys. **B706**, 487(E) (2005).

[14] Nima Arkani-Hamed and Savas Dimopoulos, Supersymmetric unification without low energy supersymmetry and signatures for fine-tuning at the LHC, J. High Energy Phys. 06 (2005) 073.

[15] Asimina Arvanitaki, Nathaniel Craig, Savas Dimopoulos, and Giovanni Villadoro, Mini-split, J. High Energy Phys. 02 (2013) 126.

[16] Nima Arkani-Hamed, Arpit Gupta, David E. Kaplan, Neal Weiner, and Tom Zorawski, Simply unnatural supersymmetry, arXiv:1212.6971.

[17] Lawrence J. Hall and Yasunori Nomura, Spread supersymmetry, J. High Energy Phys. 01 (2012) 082.

[18] Nathaniel Craig, Naturalness: A snowmass white paper, in *2022 Snowmass Summer Study* (2022), arXiv:2205.05708.

[19] F. Gabbiani, E. Gabrielli, A. Masiero, and L. Silvestrini, A Complete analysis of FCNC and *CP* constraints in general SUSY extensions of the standard model, Nucl. Phys. **B477**, 321 (1996).

[20] Wolfgang Altmannshofer, Roni Harnik, and Jure Zupan, Low energy probes of PeV scale sfermions, J. High Energy Phys. 11 (2013) 202.

[21] Cari Cesarotti, Qianshu Lu, Yuichiro Nakai, Aditya Parikh, and Matthew Reece, Interpreting the electron EDM constraint, J. High Energy Phys. 05 (2019) 059.

[22] Natsumi Nagata and Satoshi Shirai, Higgsino dark matter in high-scale supersymmetry, J. High Energy Phys. 01 (2015) 029.

[23] Scott D. Thomas and James D. Wells, Phenomenology of Massive Vectorlike Doublet Leptons, Phys. Rev. Lett. **81**, 34 (1998).

[24] Junji Hisano, Koji Ishiwata, Natsumi Nagata, and Tomohiro Takesako, Direct detection of electroweak-interacting dark matter, J. High Energy Phys. 07 (2011) 005.

[25] Richard J. Hill and Mikhail P. Solon, WIMP-Nucleon Scattering with Heavy WIMP Effective Theory, Phys. Rev. Lett. **112**, 211602 (2014).

[26] Richard J. Hill and Mikhail P. Solon, Standard Model anatomy of WIMP dark matter direct detection I: Weak-scale matching, Phys. Rev. D **91**, 043504 (2015).

[27] Richard J. Hill and Mikhail P. Solon, Standard Model anatomy of WIMP dark matter direct detection II: QCD analysis and hadronic matrix elements, Phys. Rev. D **91**, 043505 (2015).

[28] Salvatore Bottaro, Dario Buttazzo, Marco Costa, Roberto Franceschini, Paolo Panci, Diego Redigolo, and Ludovico Vittorio, The last Complex WIMPs standing, Eur. Phys. J. C **82**, 992 (2022).

[29] Marco Cirelli, Nicolao Fornengo, and Alessandro Strumia, Minimal dark matter, Nucl. Phys. **B753**, 178 (2006).

[30] H. Abdallah *et al.* (HESS Collaboration), Search for $\gamma$-Ray Line Signals from Dark Matter Annihilations in the Inner Galactic Halo from 10 Years of Observations with H.E.S.S., Phys. Rev. Lett. **120**, 201101 (2018).

[31] Alessandro Montanari, Emmanuel Moulin, and Denys Malyshev (H.E.S.S. Collaboration), Search for dark matter annihilation signals from the Galactic Center with the H.E.S.S. Inner Galaxy Survey, Proc. Sci., ICRC2021 (**2021**) 511 [arXiv:2108.10302].

[32] Lucia Rinchiuso, Oscar Macias, Emmanuel Moulin, Nicholas L. Rodd, and Tracy R. Slatyer, Prospects for detecting heavy WIMP dark matter with the cherenkov telescope array: The wino and higgsino, Phys. Rev. D **103**, 023011 (2021).

[33] Rodolfo Capdevilla, Federico Meloni, Rosa Simoniello, and Jose Zurita, Hunting wino and higgsino dark matter at the muon collider with disappearing tracks, J. High Energy Phys. 06 (2021) 133.

[34] Nima Arkani-Hamed, Tao Han, Michelangelo Mangano, and Lian-Tao Wang, Physics opportunities of a 100 TeV proton–proton collider, Phys. Rep. **652**, 1 (2016).

[35] A. Abada *et al.* (FCC Collaboration), FCC physics opportunities: Future circular collider conceptual design report volume 1, Eur. Phys. J. C **79**, 474 (2019).

[36] Philip F Hopkins *et al.*, FIRE-2 simulations: Physics versus numerics in galaxy formation, Mon. Not. R. Astron. Soc. **480**, 800 (2018).

[37] Daniel McKeown, James S. Bullock, Francisco J. Mercado, Zachary Hafen, Michael Boylan-Kolchin, Andrew Wetzel, Lina Necib, Philip F. Hopkins, and Sijie Yu, Amplified J-factors in the Galactic Centre for velocity-dependent dark

matter annihilation in FIRE simulations, Mon. Not. R. Astron. Soc. **513**, 55 (2022).

[38] Timothy Cohen, Kohta Murase, Nicholas L. Rodd, Benjamin R. Safdi, and Yotam Soreq, $\gamma$-ray Constraints on Decaying Dark Matter and Implications for IceCube, Phys. Rev. Lett. **119**, 021102 (2017).

[39] K. M. Gorski, Eric Hivon, A. J. Banday, B. D. Wandelt, F. K. Hansen, M. Reinecke, and M. Bartelman, HEALPix—A Framework for high resolution discretization, and fast analysis of data distributed on the sphere, Astrophys. J. **622**, 759 (2005).

[40] Lisa Goodenough and Dan Hooper, Possible evidence for dark matter annihilation in the inner Milky Way from the fermi gamma ray space telescope, arXiv:0910.2998.

[41] Dan Hooper and Lisa Goodenough, Dark matter annihilation in the galactic center as seen by the fermi gamma ray space telescope, Phys. Lett. B **697**, 412 (2011).

[42] Dan Hooper and Tim Linden, On the origin of the gamma rays from the galactic center, Phys. Rev. D **84**, 123005 (2011).

[43] Kevork N. Abazajian and Manoj Kaplinghat, Detection of a gamma-ray source in the galactic center consistent with extended emission from dark matter annihilation and concentrated astrophysical emission, Phys. Rev. D **86**, 083511 (2012).

[44] Tansu Daylan, Douglas P. Finkbeiner, Dan Hooper, Tim Linden, Stephen K. N. Portillo, Nicholas L. Rodd, and Tracy R. Slatyer, The characterization of the gamma-ray signal from the central Milky Way: A case for annihilating dark matter, Phys. Dark Universe **12**, 1 (2016).

[45] M. Ackermann *et al.* (Fermi-LAT Collaboration), The fermi galactic center GeV excess and implications for dark matter, Astrophys. J. **840**, 43 (2017).

[46] Tim Linden, Nicholas L. Rodd, Benjamin R. Safdi, and Tracy R. Slatyer, The high-energy tail of the galactic center gamma-ray excess, Phys. Rev. D **94**, 103013 (2016).

[47] S. Abdollahi *et al.* (Fermi-LAT Collaboration), *Fermi* large area telescope fourth source catalog, Astrophys. J. Suppl. Ser. **247**, 33 (2020).

[48] S. Abdollahi *et al.*, Incremental fermi large area telescope fourth source catalog, Astrophys. J. Suppl. Ser. **260**, 53 (2022).

[49] See Supplemental Material at http://link.aps.org/supplemental/10.1103/PhysRevLett.130.201001 for details of our methods, extended results, and systematic tests of our analysis, which includes Ref. [50–57].

[50] M. Ackermann *et al.* (Fermi-LAT Collaboration), Searching for Dark Matter Annihilation from Milky Way Dwarf Spheroidal Galaxies with Six Years of Fermi Large Area Telescope Data, Phys. Rev. Lett. **115**, 231301 (2015).

[51] Glen Cowan, Kyle Cranmer, Eilam Gross, and Ofer Vitells, Asymptotic formulae for likelihood-based tests of new physics, Eur. Phys. J. C **71**, 1554 (2011); Eur. Phys. J. C **73**, 2501(E) (2013).

[52] Matthew Baumgart, Ira Z. Rothstein, and Varun Vaidya, On the Annihilation Rate of WIMPs, Phys. Rev. Lett. **114**, 211301 (2015).

[53] Marco Cirelli, Alessandro Strumia, and Matteo Tamburini, Cosmology and astrophysics of minimal dark matter, Nucl. Phys. **B787**, 152 (2007).

[54] Junji Hisano, Shigeki. Matsumoto, Mihoko M. Nojiri, and Osamu Saito, Non-perturbative effect on dark matter annihilation and gamma ray signature from galactic center, Phys. Rev. D **71**, 063528 (2005).

[55] Jatan Buch, Marco Cirelli, Gaëlle Giesen, and Marco Taoso, PPPC 4 DM secondary: A poor particle physicist Cookbook for secondary radiation from Dark Matter, J. Cosmol. Astropart. Phys. 09 (2015) 037.

[56] Francesca Calore, Ilias Cholis, and Christoph Weniger, Background model systematics for the Fermi GeV excess, J. Cosmol. Astropart. Phys. 03 (2015) 038.

[57] Malte Buschmann, Nicholas L. Rodd, Benjamin R. Safdi, Laura J. Chang, Siddharth Mishra-Sharma, Mariangela Lisanti, and Oscar Macias, Foreground mismodeling and the point source explanation of the fermi galactic center excess, Phys. Rev. D **102**, 023023 (2020).

[58] Marco Cirelli, Gennaro Corcella, Andi Hektor, Gert Hutsi, Mario Kadastik, Paolo Panci, Martti Raidal, Filippo Sala, and Alessandro Strumia, PPPC 4 DM ID: A poor particle physicist cookbook for dark matter indirect detection, J. Cosmol. Astropart. Phys. 03 (2011) 051; J. Cosmol. Astropart. Phys.10 (2012) E01.

[59] Julio F. Navarro, Carlos S. Frenk, and Simon D. M. White, The structure of cold dark matter halos, Astrophys. J. **462**, 563 (1996).

[60] Julio F. Navarro, Carlos S. Frenk, and Simon D. M. White, A Universal density profile from hierarchical clustering, Astrophys. J. **490**, 493 (1997).

[61] Henry W. Leung, Jo Bovy, J. Ted Mackereth, Jason A. S. Hunt, Richard R. Lane, and John C. Wilson, A direct measurement of the distance to the Galactic center using the kinematics of bar stars, Mon. Not. R. Astron. Soc. **519**, 948 (2022).

[62] Pablo F. de Salas and Axel Widmark, Dark matter local density determination: recent observations and future prospects, Rep. Prog. Phys. **84**, 104901 (2021).

[63] Martin Beneke, Caspar Hasner, Kai Urban, and Martin Vollmann, Precise yield of high-energy photons from Higgsino dark matter annihilation, J. High Energy Phys. 03 (2020) 030.

[64] Matthew Baumgart, Timothy Cohen, Emmanuel Moulin, Ian Moult, Lucia Rinchiuso, Nicholas L. Rodd, Tracy R. Slatyer, Iain W. Stewart, and Varun Vaidya, Precision photon spectra for wino annihilation, J. High Energy Phys. 01 (2019) 036.

[65] Christopher Dessert, Joshua W. Foster, Yujin Park, Benjamin R. Safdi, and Weishuang Linda Xu, https://github.com/bsafdi/higgsino_confronts_14 years_fermi_data (2023).